

Dissipative dark-bright vector solitons in fiber lasersX. Hu,¹ J. Guo,² G. D. Shao,¹ Y. F. Song,¹ L. M. Zhao,² L. Li,² and D. Y. Tang^{1,*}¹*School of Electrical and Electronic Engineering, Nanyang Technological University, Singapore*²*Jiangsu Key Laboratory of Laser Materials and Devices, School of Physics and Electronic Engineering, Jiangsu Normal University, Xuzhou, China*

(Received 13 March 2020; accepted 12 May 2020; published 2 June 2020)

We present detailed studies on dark-bright vector solitons formed in dispersion- and birefringence-managed fiber lasers sustained by either incoherent or coherent cross-polarization coupling. We show that even under strong influence of the gain bandwidth limitation, coupled dark-bright solitons can still be formed in a fiber laser. Unique features of the dissipative dark-bright vector solitons are studied both numerically and experimentally, and compared with those of the vector solitons formed in nonlinear Schrödinger equation systems.

DOI: [10.1103/PhysRevA.101.063807](https://doi.org/10.1103/PhysRevA.101.063807)**I. INTRODUCTION**

Recently, we reported experimental observation of dark-bright vector solitons in weakly birefringent cavity fiber lasers and showed that the features of the observed dark-bright vector solitons could be well described by the coupled nonlinear Schrödinger equations (NLSEs) [1,2]. Formation of dark-bright vector solitons in single mode fibers was theoretically extensively investigated previously; e.g., Christodoulides theoretically predicted formation of dark-bright vector solitons in single mode fibers under coherent cross-polarization coupling [3] and Lisak *et al.* investigated the dark-bright vector soliton formation under incoherent cross-polarization coupling [4]. Theoretical studies have shown that cross-polarization modulation played a critical role in the dark-bright vector soliton formation [3,4]. Different from the scalar soliton formation in single mode fibers, where bright solitons can only be formed in the anomalous dispersion regime, and dark solitons in the normal fiber dispersion regime, the formation of dark-bright vector solitons is independent of the sign of fiber dispersion. However, it is a challenge to obtain experimentally dark-bright vector solitons in the conventional single mode fibers. As analyzed theoretically, in order for the dark-bright vector solitons to be formed in a single mode fiber, both the fiber dispersion and birefringence at the soliton frequencies have to fulfill certain stringent requirements or relations [3–8]. It is difficult for these requirements or relations to be fulfilled by the conventional single mode fibers. Therefore, despite the extensive theoretical studies on the topic, few experimental observations on the type of vector solitons have been reported. To overcome the difficulties, we have found an innovative solution: Instead of propagating light in a piece of single mode fiber we let light circulate in an appropriately designed fiber ring laser. As the dynamics of light circulation in such a fiber ring laser is mainly determined by the averaged fiber parameters over the entire cavity [9], through cavity dispersion and birefringence management one could practically get

access to any desired fiber dispersion and birefringence parameters. Consequently, we could experimentally successfully demonstrate both the coherently and incoherently coupled dark-bright vector solitons in single mode fibers.

Strictly speaking, the dynamics of light circulation in a fiber laser cavity is physically different from that of light propagation in a fiber transmission line. In a fiber laser cavity, in addition to the nonlinear propagation in the single mode cavity fibers, other effects, such as the laser gain and losses, gain saturation, and gain bandwidth limitation also exist and should be considered. These effects could unavoidably affect the dynamics of the light propagation in the cavity fibers and the properties of the formed solitons. What are the influences of these effects on the dark-bright vector soliton formation? It is known that under the existence of strong effective gain bandwidth limitation, the equation that describes the light circulation in a fiber laser cavity is no longer mathematically equivalent to the NLSE. Solitons formed in such a fiber laser are typical dissipative solitons [10,11]. Could dissipative dark-bright vector solitons be formed and remain stable in such a fiber laser? What are the characteristics of the dissipative dark-bright vector solitons and how are they different from those of the NLSE type of dark-bright vector solitons? All these questions are so far not addressed.

To answer the above questions, we have investigated both numerically and experimentally the dark-bright vector soliton formation in single mode fiber lasers under different cavity parameters and laser operation conditions. In this paper, we present the detailed results of our studies.

II. NUMERICAL SIMULATIONS

We have numerically modeled the dark-bright vector soliton formation in fiber lasers with different cavity parameters and studied properties of the formed vector solitons. In order to make the simulation results directly comparable with the experimental observations, our simulations were conducted based on a real experimental fiber laser configuration. Specifically, we consider a fiber ring laser whose ring cavity is made of 3-m Er-doped fiber (EDF) with normal

*Corresponding author: edytang@ntu.edu.sg

Group-velocity dispersion (GVD) of $61.18 \text{ ps}^2/\text{km}$, and different lengths of dispersion-compensating fiber (DCF) with GVD of $5.1 \text{ ps}^2/\text{km}$, and single mode fiber (SMF) with GVD of $-22.94 \text{ ps}^2/\text{km}$. Both the SMF and DCF fibers are used because through selecting appropriate DCF and SMF lengths, the desired average cavity GVD as well as cavity length can be obtained. We assume that the birefringence axes of the fibers used in constructing the cavity are aligned with each other. Moreover, we adopted a so-called pulse tracing technique to simulate the laser operation [12]. Briefly, we start the numerical simulations with a weak initial dark-bright pulse pair and let them circulate in the fiber laser cavity. The light propagation in the gain fiber is described by the coupled extended Ginzburg-Landau equations (GLEs):

$$\begin{aligned} \frac{\partial u}{\partial z} &= i\beta u - \delta \frac{\partial u}{\partial t} - \frac{i\beta_{2u}}{2} \frac{\partial^2 u}{\partial t^2} \\ &\quad + i\gamma \left(|u|^2 + \frac{2}{3}|v|^2 \right) u + \frac{i\gamma}{3} v^2 u^* + \frac{g}{2} u + \frac{g}{2\Omega_g^2} \frac{\partial^2 u}{\partial t^2}, \\ \frac{\partial v}{\partial z} &= -i\beta v + \delta \frac{\partial v}{\partial t} - \frac{i\beta_{2v}}{2} \frac{\partial^2 v}{\partial t^2} \\ &\quad + i\gamma \left(|v|^2 + \frac{2}{3}|u|^2 \right) v + \frac{i\gamma}{3} u^2 v^* + \frac{g}{2} v + \frac{g}{2\Omega_g^2} \frac{\partial^2 v}{\partial t^2}, \end{aligned} \quad (1)$$

where u and v are the normalized envelopes of the optical fields along the two orthogonal polarization modes of the fiber. $2\beta = 2\pi\Delta n/\lambda$ is the wave-number difference between the modes and $2\delta = 2\beta\lambda/2\pi c$ is the inverse group velocity difference. β_{2u} and β_{2v} are the second-order dispersion coefficients along the two orthogonal axes, and γ represents the nonlinearity of the fiber, g is the saturable gain coefficient of the gain fiber, and Ω_g is the gain bandwidth. For the light propagation in the undoped fibers, $g = 0$. In our simulations, the gain saturation is described by

$$g = g_0 \exp \left[-\frac{\int (|u|^2 + |v|^2) dt}{E_{\text{sat}}} \right], \quad (2)$$

where g_0 is the small signal gain coefficient and E_{sat} is the saturation energy. When the light meets the cavity output port, 10% of the light intensity is deducted from the light fields, and the rest of the light is then reinjected into the cavity as the input for the next round of cavity circulation. We used the standard split-step method to solve the coupled extended GLEs (1). The numerical calculations were made on a 400-ps window and the periodic boundary condition was used. In our simulations, whenever possible, we used the real fiber parameters. We note that our simulation technique has automatically considered the cavity dispersion and birefringence management. In addition, the group velocity mismatching is also included in the simulation. Using the same model and numerical simulation technique we have previously successfully reproduced almost all soliton features experimentally observed in fiber lasers, such as coherent energy exchange between vector soliton components [13], noiselike pulse emission [14], soliton quantization effect [12], and soliton-period-doubling route to chaos [15]. In the current simulations, we are interested in the dark-bright vector soliton formation and

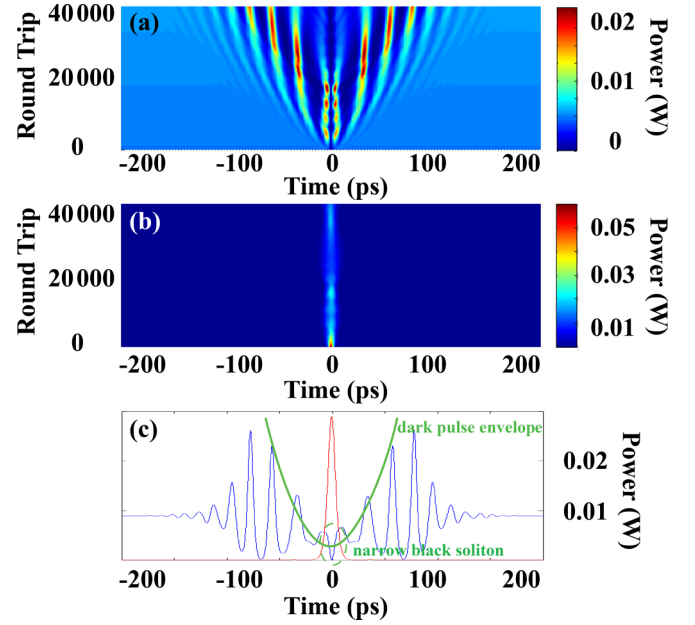


FIG. 1. Coherently coupled dark-bright solitary waves in the net anomalous dispersion regime. The initial envelopes of the dark and bright pulse field are $u = 0.1 \tanh(0.5t)$ and $v = 0.1 \text{sech}(0.5t)$; (a) evolution of the dark pulse along the cavity round trips; (b) evolution of the bright pulse along the cavity round trips; (c) the coupled dark-bright pulses at the cavity round trip of 40 000.

their dynamics in fiber lasers, as well as the influences of the effective gain bandwidth limitation on the properties of the formed dark-bright vector solitons. To this end we have focused our numerical studies on either the coherent cross-polarization coupling (XPC) or incoherent XPC cases.

A. Coherent XPC case

We first considered fiber lasers with very weak net cavity birefringence. When the net linear cavity birefringence is sufficiently small, the coupling between the two orthogonal polarization components of the laser emission is coherent. In all of our simulations we have set the initial slowly varying envelope of the dark and bright pulse fields as $u = A \tanh(Bt)$ and $v = C \text{sech}(Bt)$, where A , C , and B are arbitrary constants and stand for the bright soliton strength, the dark soliton depth, and the soliton pulse width, respectively. The initial pulse widths of the dark and bright solitons are set equal.

For lasers with cavity dispersion in the anomalous dispersion regime, we used a set of the following parameters: EDF fiber gain bandwidth: $\Omega_g = 50 \text{ nm}$; small signal gain coefficient: $g_0 = 100 \text{ km}^{-1}$; gain saturation energy $E_{\text{sat}} = 1 \text{ pJ}$; EDF length: 3 m; DCF length: 2 m; SMF length: 9 m. The birefringence beat lengths of the cavity fibers are 50 km (EDF), 100 km (SMF), and 150 km (DCF), respectively. Thus, the average fiber group velocity mismatch is $\delta_{\text{ave}} = 3.0139 \times 10^{-5} \text{ ps/km}$, and the averaged fiber dispersions for the bright and dark solitons are $\beta_{2u} = \beta_{2v} = -0.91 \text{ ps}^2/\text{km}$.

A typical result obtained under the laser parameters is shown in Fig. 1. After an initial pulse shaping process, a dark-bright pulse pair is formed in the fiber laser. The pulse

pairs propagate stably with the cavity round trips, suggesting that they are a kind of solitary wave of the laser. We note that the dark solitary pulse in Fig. 1 is embedded in a train of cw background pulses and always has zero minimum intensity. Such a dark soliton is also known as a black soliton. According to [3], black-white vector solitons can be formed in a weakly birefringent fiber under coherent XPC. The numerical result shows that under appropriate laser cavity and operation conditions, under coherent XPC stable black-white vector solitons could be formed even in a fiber laser, despite the fact that light circulation in a fiber laser cavity is not exactly the same as that of light propagation in a SMF.

In the current simulation, we used an effective gain bandwidth of 50 nm, which is far broader than the spectral bandwidths of the formed solitons. When the gain bandwidth is far larger than the soliton spectral bandwidth, one could effectively neglect the gain-bandwidth-limitation effect. As in the steady-state operation of a laser, the saturated gain is always balanced by the cavity losses; in this case the extended GLE describing the fiber laser operation could mathematically be reduced to the NLSE [16]. Therefore, it is expected that solitons formed in such a fiber laser would mimic the NLSE soliton dynamics. To check this, we also numerically simulated the dark-bright vector soliton formation in coherently coupled NLSEs without considering the cavity dispersion- and birefringence-management and gain saturation under the same fiber parameters and compared the results. They exhibit similar features, such as the formation of a stable dark-bright vector state is critically dependent on the appropriate selection of the initial dark-bright pulse parameters. In the net anomalous cavity dispersion regime, modulation instability (MI) always occurred on the cw component [17]. Therefore, the cw background intensity became strongly modulated, as shown in Fig. 1. However, we note that due to the cavity boundary condition, the MI induced intensity modulation always evolves to a stable periodic pulse pattern on top of a weak cw background in a laser cavity. Depending on the cw background strength, the repetition rate and pulse intensity of the periodic pulse pattern vary, but the occurrence of MI would neither prevent the black-white vector soliton formation nor destroy it, as shown in Fig. 1 by the dash-circled part. This is very different from the dark-bright vector soliton formation in SMFs where the occurrence of MI eventually destroys the formed dark-bright vector solitons [18]. A challenge for the experimental study on dark solitons is to detect their existence. Unlike the bright solitons, which are intensity peaks that can be easily detected even with a slow detector, a dark soliton is an intensity dip embedded in a cw intensity background. If a dark soliton is too weak or has a too narrow pulse width, it is difficult to detect its existence even with a high-speed detection system. An interesting feature uncovered by the numerical simulation is that associated with the narrow dark soliton formation as shown in the dashed circle in Fig. 1(c), the peaks of the MI pulses also form a dark pulse envelope due to the XPC, indicated in the thick line in Fig. 1(c). The dark pulse envelope is much broader than the formed dark soliton. Obviously, the formation of such a dark pulse peak envelope would greatly facilitate the detection of the narrow dark soliton formed in an experiment.

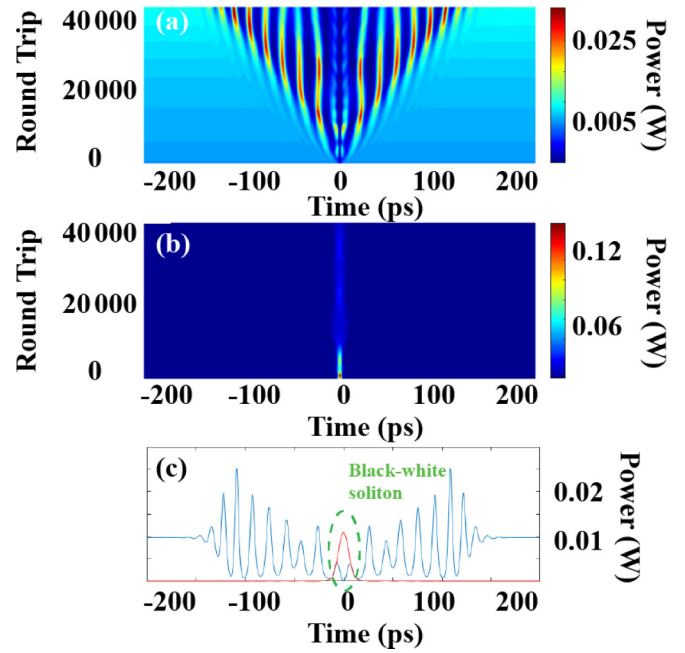


FIG. 2. Same as in Fig. 1, except the small signal gain coefficient is changed to $g_0 = 150 \text{ km}^{-1}$ and laser gain bandwidth is changed to 20 nm.

To study the influence of the gain bandwidth limitation on the dark-bright vector soliton formation, we then set the gain bandwidth $\Omega_g = 20 \text{ nm}$ and the small signal gain coefficient $g_0 = 150 \text{ km}^{-1}$; the result obtained is shown in Fig. 2. Stable coherently coupled dark-bright solitons can still be formed in such a fiber laser. However, compared with the results obtained under negligible gain bandwidth, we numerically identified that the formation of the dark-bright vector solitons is more robust. At a fixed gain and saturation energy, independent of the initial pulse parameter selections, the same dark-bright vector soliton is always automatically obtained, which is a typical feature of the dissipative solitons [19,20].

For lasers in the net normal cavity dispersion regime, we used the following parameters: EDF gain bandwidth: $\Omega_g = 50 \text{ nm}$, small signal gain coefficient: $g_0 = 400 \text{ km}^{-1}$; EDF length: 3 m; DCF length: 5 m; SMF length: 8 m. Thus, the average GVD at the bright and dark soliton frequency is $\beta_{2u} = \beta_{2v} = 1.6 \text{ ps}^2/\text{km}$. We have kept the same net average group velocity mismatching $\delta_{ave} = 3.0139 \times 10^{-5} \text{ ps}/\text{km}$.

The result obtained in the case is shown in Fig. 3. In the normal dispersion regime, there is no MI effect. Hence, the cw has a stable background. Again, with appropriate initial pulse parameter selection, stable coherently coupled dark-bright solitons are formed in the laser, showing that the dark-bright vector soliton formation is independent of the sign of the laser cavity dispersion. However, different from the case of the dark-bright vector soliton formation in the net anomalous dispersion regime, in addition to the initial dark-bright pulse pair, two extra dark-bright vector solitons are also formed. To explain this, we note that the formation of dark solitons has no dark pulse intensity threshold in the normal dispersion fibers [18]. Any small intensity dip on a cw background could evolve into one or multiple dark solitons under strong

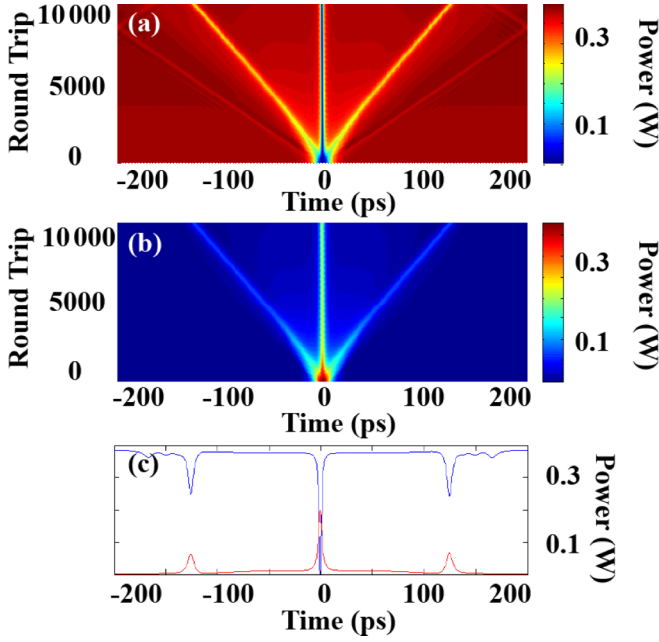


FIG. 3. Coherently coupled dark-bright solitons in the net normal dispersion regime. The initial optical fields are set as $u = 0.1 \tanh(0.5t)$ and $v = 0.1 \operatorname{sech}(0.5t)$; (a) evolution of dark solitons; (b) evolution of bright solitons; (c) coupled dark-bright soliton at the simulation round trip of 10 000.

light intensity. As the initial pulses used are not the stable dark-bright vector soliton, they would certainly experience nonlinear pulse shaping and generate new solitons. However, interestingly, associated with each of the newly formed dark solitons, a bright soliton is also formed and copropagates with the dark solitons. The result suggests that formation of the coupled dark-bright vector solitons could be an intrinsic feature of the fiber lasers under coherent XPC. The two counterpropagating dark and bright solitons are symmetric. They have the same pulse width and peak intensity, which is the typical characteristic of the vector solitons formed. To study the influence of the gain bandwidth limitation on the dark-bright solitons in the dispersion regime, we further set the laser gain bandwidth to 20 nm and the gain coefficient to $g_0 = 400 \text{ km}^{-1}$. The result is displayed in Fig. 4. As expected, except that the dark soliton depth is enhanced and the formation of the dark-bright vector soliton becomes more robust, no other obvious difference could be numerically detected from those of the dark-bright vector solitons formed under the negligible gain-bandwidth-limitation case.

B. Incoherent XPC case

When the net linear cavity birefringence is sufficiently large, the laser oscillations along the two orthogonal polarization directions will have different frequencies. Consequently, the coupling between them is incoherent. To simulate fiber laser operation under incoherent XPC in the anomalous dispersion regime, we used the following set of parameters: EDF fiber gain bandwidth: $\Omega_g = 20 \text{ nm}$; small signal gain coefficient: $g_0 = 150 \text{ km}^{-1}$; gain saturation energy $E_{\text{sat}} = 1 \text{ pJ}$; EDF: 3 m; SMF: 9 m; DCF: 2 m. The beat lengths of the fibers

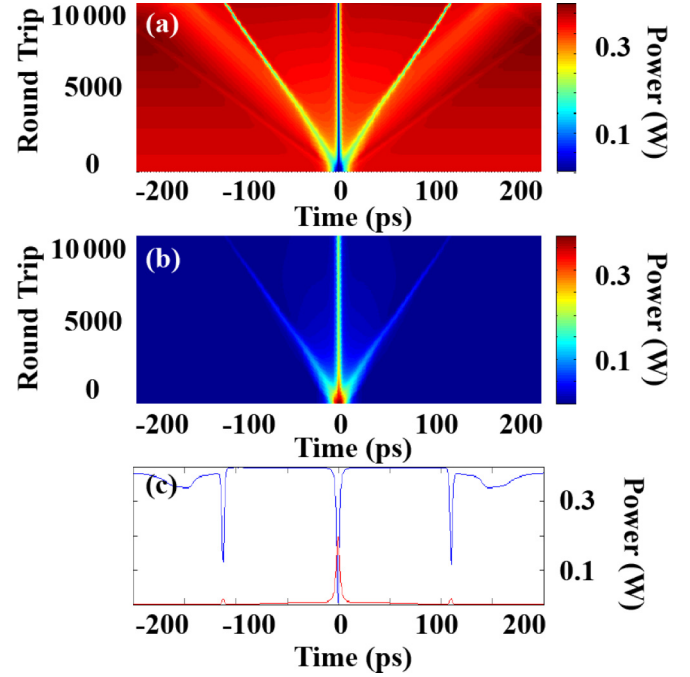


FIG. 4. The same as in Fig. 3, except the laser gain bandwidth changed to 20 nm.

are 10 m (EDF), 20 m (SMF), and 30 m (DCF), respectively. Thus, the average group velocity mismatch is 0.14 ps/km , the averaged GVDs for the bright and dark solitons are $\beta_{2v} = -0.91 \text{ ps}^2/\text{km}$, and $\beta_{2u} = -0.91 \text{ ps}^2/\text{km}$, respectively.

Figure 5 shows the obtained numerical result. Comparing with Fig. 1, although the same initial pulse parameters were used, due to the incoherent XPC and the large cavity

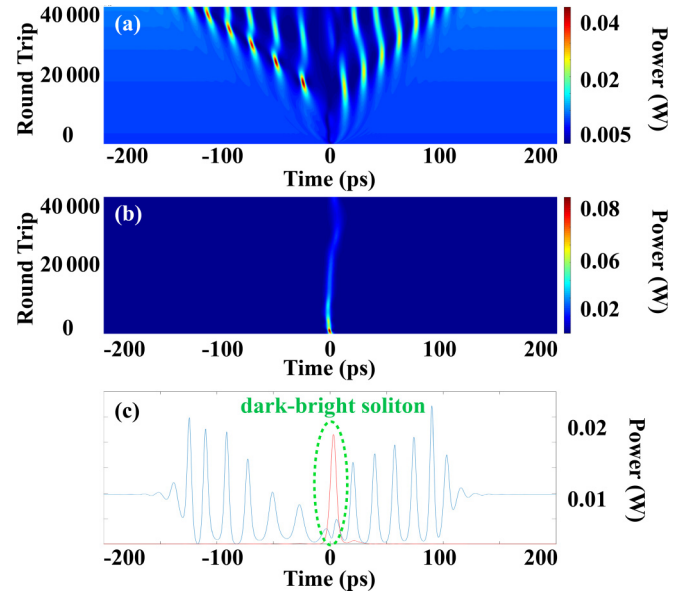


FIG. 5. Incoherently coupled dark-bright solitons in the net anomalous dispersion regime. Initial optical fields along the two axes: $u = 0.1 \tanh(0.5t)$ and $v = 0.1 \operatorname{sech}(0.5t)$; (a) evolution of dark solitons; (b) evolution of bright solitons; (c) coupled dark-bright soliton at simulation round trip of 40 000.

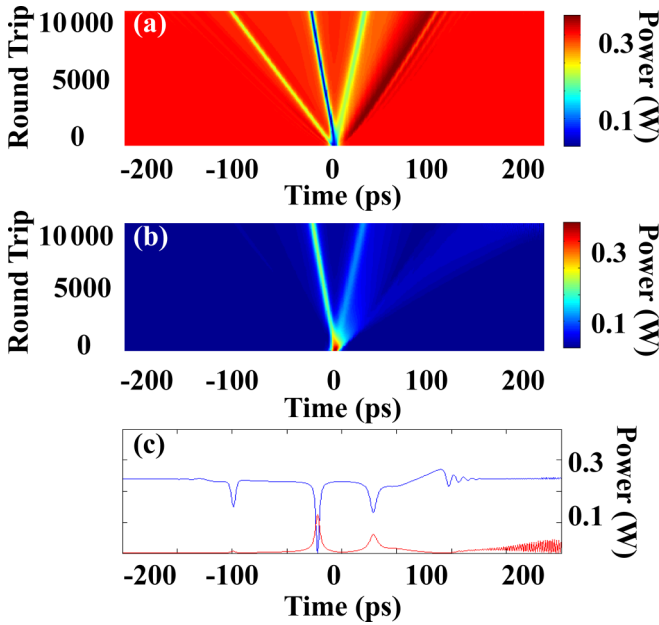


FIG. 6. Incoherently coupled dark-bright solitons in the net normal dispersion regime. (a) Evolution of dark solitons; (b) evolution of bright solitons; (c) coupled dark-bright soliton at simulation round trip of 10000.

birefringence, the formed dark soliton depth did not reach zero intensity. Moreover, the pulse peak modulation of the MI pulses is no longer symmetric with respect to the bright solitons. Based on extensive numerical simulations we confirmed that, similar to the incoherently coupled NLSE systems [4], as far as the dispersion condition $(2/3)\beta_{2u} < \beta_{2v}$ is fulfilled, dissipative dark-bright vector solitons could always be formed in the dispersion regime, while if the dispersion condition is not fulfilled, no stable dissipative dark-bright vector solitons could be formed.

To check the incoherently coupled dark-bright vector soliton formation in the net normal dispersion regime, we first used the following parameters: EDF gain bandwidth $\Omega_g = 50$ nm; small signal gain coefficient $g_0 = 400$ km⁻¹; saturation energy $E_s = 10$ pJ; EDF: 3 m; SMF: 8 m, DCF: 5 m. To also take into account the different GVDs of the dark and bright solitons under the incoherent coupling, we deliberately set the dispersion coefficient of the SMF for the dark and bright soliton as -22.94 and -24.22 ps²/km, respectively. This results in the average fiber dispersion for the dark and bright solitons being $\beta_{2u} = 1.6$ and $\beta_{2v} = 0.96$ ps²/km. We have set the beat length of the fibers as 6 m (EDF), 12 m (SMF), and 18 m (DCF), respectively, which then makes the averaged group velocity mismatch 0.28 ps/km.

Figure 6 shows the result obtained. Multiple pairs of dark-bright solitons are simultaneously formed. Due to the large fiber birefringence, the group velocity mismatch becomes obvious; as a result, the formed dark-bright vector solitons have different pulse widths and pulse heights. As mentioned above, when the gain-bandwidth-limitation effect is negligible, in a steady state the formed solitons in a fiber laser mimic the NLSE soliton features. A typical feature of the incoherently coupled NLSE type dark-bright vector solitons is that a stronger bright

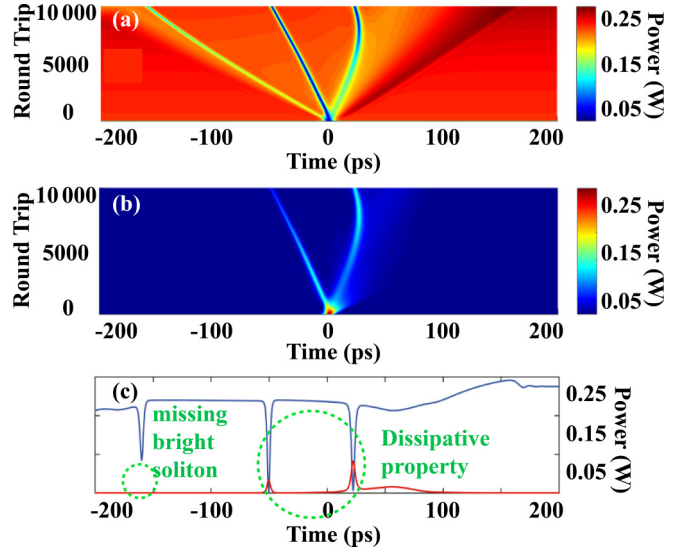


FIG. 7. The same as in Fig. 6, except the laser gain bandwidth is changed to 20 nm.

soliton is always coupled to a deeper dark soliton. We call it an “attractive feature” of the coupled dark-bright solitons. As can be seen in Fig. 6, the numerical result clearly reflects the feature. Here it is worth making a comparison with the result shown in Fig. 3. In both cases multiple coupled dark-bright solitons can be simultaneously formed in a fiber laser. While under the coherent XPC the newly formed dark-bright vector solitons always exhibit the same pulse width and height; under incoherent XPC, the newly formed dark-bright vector solitons could have different pulse widths and energies, which makes the dark-bright vector solitons formed under the two XPC cases distinguishable.

To identify properties of the dissipative dark-bright vector solitons formed under incoherent XPC, we then set the gain bandwidth to 20 nm and repeated the simulation. The result is displayed in Fig. 7. Despite the fact that the formed dark-bright vector solitons still have different pulse widths and pulse heights, it can be seen that under the gain bandwidth limitation, a stronger bright soliton could also couple to a weaker dark soliton, demonstrating that the incoherently coupled dissipative dark-bright vector solitons no longer possess the “attractive property.” Moreover, as shown in Fig. 7, in the case a dark soliton could even exist alone, without coupling to a bright soliton.

III. EXPERIMENTAL OBSERVATIONS

To check the numerical simulations, we further constructed fiber lasers with comparable net average cavity dispersions and birefringence to investigate the dark-bright vector soliton formation and their features. All the fiber lasers have the same cavity structure as shown in Fig. 8, and the same 3-m Er-doped fiber with normal GVD of 61.18 ps²/km as the gain fiber. The other cavity fibers used are SMF with a GVD of -22.94 ps²/km and DCF with a GVD of 5.1 ps²/km. Through appropriately selecting the lengths of the SMF and DCF we managed to get the desired average fiber GVD, birefringence, and the cavity length. The fiber lasers are

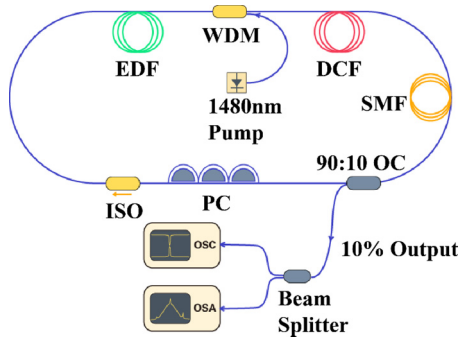


FIG. 8. A schematic of the Er-doped fiber (EDF) ring laser. SMF: Single mode fiber. DCF: Dispersion-compensating fiber. WDM: Wavelength division multiplexer. PC: Polarization controller. ISO: Isolator. OC: Output coupler. OSC: Oscilloscope.

pumped by a 1480-nm SMF Raman laser that has a maximum output power of ~ 5 W. A polarization-independent isolator is inserted in the cavity to force the unidirectional light circulation. An intracavity polarization controller (PC) is used to fine-tune the linear cavity birefringence. A wavelength division multiplexer (WDM) is used to couple the pump light into the cavity, and a 10% fiber coupler is used to output the light. All the components used in the cavity are pigtailed with the DCF. No real or artificial saturable absorbers are inserted in the cavity.

When constructing the fiber cavities, special care has been taken to ensure that the net cavity birefringence is sufficiently small, so the laser can simultaneously oscillate in its two orthogonal linear polarization modes, and through carefully adjusting the intracavity PC, the net birefringence of the cavity can be varied over a small range across the zero cavity birefringence point. Experimentally, this is judged by monitoring the optical spectra of laser emissions along the two orthogonal polarization directions. As the intracavity PC orientation is tuned, they could be tuned overlapping and then separating.

We first focused on laser operation under the coherent XPC in the anomalous dispersion regime. For this purpose, we used a 9-m single mode fiber and a 2-m DCF to complete the ring cavity. The final cavity length is 14 m, and the averaged net cavity GVD is about $\beta_2 = -0.91$ ps²/km. In order to have coherent XPC, the net linear cavity birefringence must be sufficiently small. Experimentally this is very challenging to achieve. Nevertheless, through appropriately selecting the fibers and the intracavity components, and carefully tuning the intracavity PC, a state as shown in Fig. 9 could be obtained. Figure 9(a) shows the polarization resolved laser emission along the two orthogonal polarization directions of the cavity. The cavity round-trip time of our fiber laser is about 70 ns. Based on Fig. 9(a), obviously multiple coupled dark-bright pulse pairs are simultaneously formed in the laser. In particular, all the pulse pairs exhibit the same pulse heights, indicating that they could have the same pulse parameters. The soliton nature of the pulses is confirmed by their optical spectra, as shown in Fig. 9(b). Both the Kelly sidebands and the coherent energy exchange sidebands coexist on the spectra, indicating that the dark and bright pulses are solitons and they are coherently coupled [14]. In our experiment the coherently coupled dark-bright soliton operation state is very

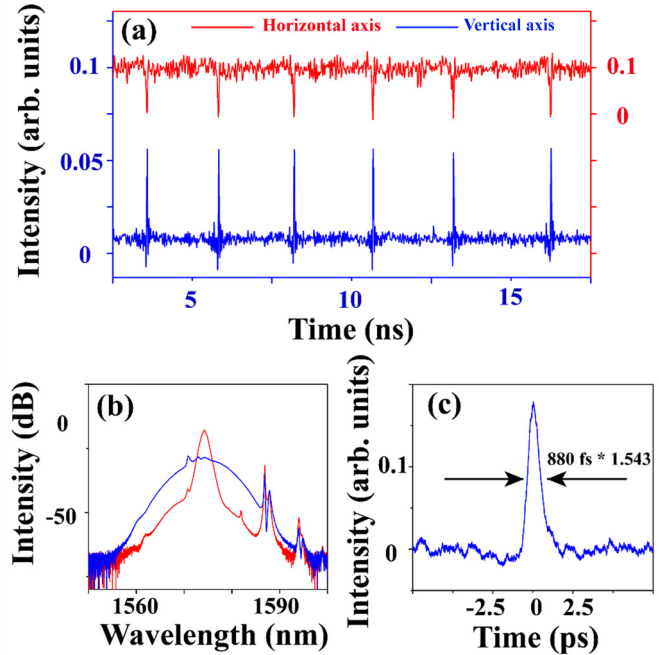


FIG. 9. (a) Coherently coupled dark-bright solitons formed in the net anomalous cavity dispersion regime. Horizontal axis (upper trace), vertical axis (lower trace); (b) corresponding optical spectra of the solitons; (c) autocorrelation trace for the bright solitons.

difficult to achieve. At a fixed pump strength, in order to observe the state, in addition to tuning the net cavity birefringence as small as possible, one has also to control the average cavity dispersion to an appropriate small value. Based on the autocorrelation measurement on the bright solitons shown in Fig. 9(c), the solitons should have a pulse width of about 880 fs if a sech^2 shape is assumed. We note that under coherent XPC, only the black-white vector solitons could be formed, and the formed solitons would have the same pulse parameters. In our experiment, the electronic detection system used only has a bandwidth of 33 GHz; theoretically it could not detect the existence of the dark solitons. However, the dark solitons were clearly observable in our experiment, as shown in Fig. 9. Based on our numerical simulations, we attribute it to the existence of the dark envelope formed on the MI pulses. Therefore, the experimental result is well supportive to the numerical simulations.

Depending on the net cavity birefringence, incoherently coupled dark-bright vector solitons can also be formed in the same fiber laser. At a large net cavity birefringence, initially the polarization domain walls can be observed. As the net cavity birefringence is decreased or the pump power is increased, the domain walls split, and eventually multiple coupled dark-bright solitons are formed in the cavity as shown in Fig. 10(a). Multiple pairs of dark-bright solitons are always initially formed within one cavity round trip. Figure 10(b) shows the corresponding polarization resolved optical spectra of the laser emission. The laser emission along the two orthogonal polarization directions obviously has different wavelengths. We note that the dark-bright vector solitons cannot be obtained in all incoherent XPC situations. If the net average cavity GVD is too large, where only the polarization

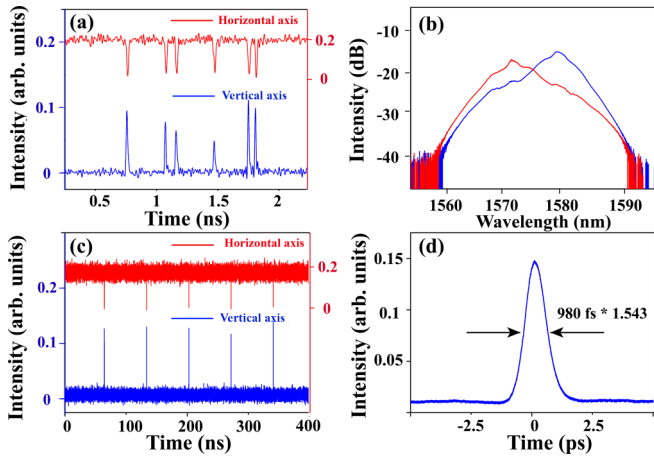


FIG. 10. (a) Incoherently coupled dark-bright solitons in the net anomalous cavity dispersion regime. Horizontal axis (upper trace), vertical axis (lower trace); (b) corresponding optical spectra; (c) single pair of dark-bright solitons propagating in the cavity; (d) autocorrelation trace for the bright solitons.

domains can be obtained, or the condition $(2/3)\beta_{2u} < \beta_{2v}$ is not fulfilled, no dark-bright solitons could be obtained. Obviously, the dark-bright vector solitons have different pulse widths and pulse energies, which are clearly different from those shown in Fig. 9(a). Through careful control of the laser operation conditions, single dark-bright vector soliton operation can also be obtained, as depicted in Fig. 10(c). The corresponding autocorrelation trace, shown in Fig. 10(d), has a FWHM autocorrelation trace width of ~ 1.5 ps, assuming the pulse has a sech^2 shape; its width is estimated to be 980 fs.

To verify the dark-bright vector soliton formation and their properties in the net normal dispersion regime, we constructed a fiber laser with an 8-m SMF and a 5-m DCF. The fiber laser has a cavity length of 16 m, corresponding to a cavity round-trip time of 80 ns. The estimated net average GVD of the cavity is $\beta_2 = 1.6 \text{ ps}^2/\text{km}$. Through carefully tuning the intracavity PC paddles, multiple dark-bright vector solitons were obtained. A typical dark-bright vector soliton emission state is shown in Fig. 11. Figure 11(a) is the polarization resolved laser emissions. Figure 11(b) is the corresponding polarization resolved optical spectra. Similar to Fig. 10(a), each bright soliton is coupled to a dark soliton, and the solitons exhibit different pulse widths and pulse energies. In particular, a weak bright soliton could couple to a deeper dark soliton, indicating that the dark-bright solitons are not only incoherently coupled but also dissipative. Extensive experimental studies have shown that only under some special laser operation conditions, e.g., strong pumping and relatively larger average cavity dispersion, the incoherently coupled dark-bright solitons exhibited the attractive feature. Generally, they do not exhibit the feature, indicating that they are dissipative dark-bright vector solitons.

Figure 12 further shows another state observed in the fiber laser. The observed dark-bright vector solitons not only do not have the attractive feature, but also a scalar dark soliton coexists with multiple incoherently coupled dark-bright vector solitons in the cavity, which further confirms that they are dissipative dark-bright vector solitons.

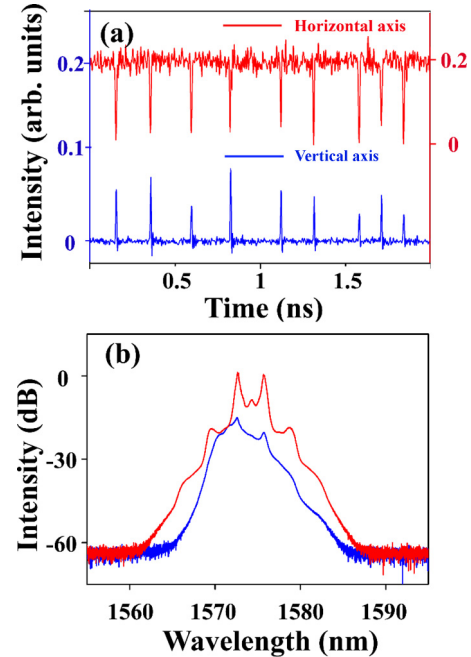


FIG. 11. (a) Incoherently coupled dark-bright solitons measured in the net normal cavity dispersion regime. Horizontal axis (upper trace), vertical axis (lower trace); (b) the corresponding optical spectra.

IV. CONCLUSION

In conclusion, we have studied both numerically and experimentally the dark-bright vector soliton formation in a single mode fiber laser operating in different parameter regimes. We have numerically shown that as a result of the XPC, stable dark-bright vector solitons can even be formed in a fiber laser independent of the sign of the net cavity dispersion. Specifically, we have studied the features of the formed dark-bright vector solitons under the coherent and incoherent XPC, and shown that under the coherent XPC black-white vector solitons were formed, while under the incoherent XPC dark-bright vector solitons with different soliton pulse parameters were formed. We also numerically investigated the influence of effective gain bandwidth on the formed dark-bright vector

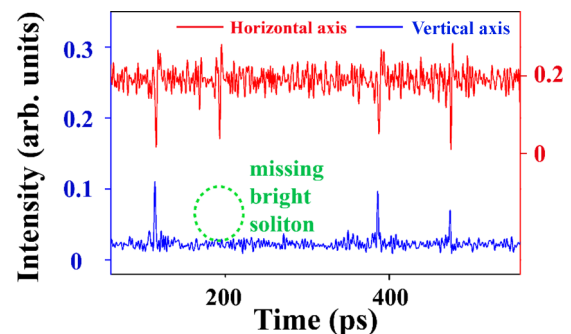


FIG. 12. A state of the laser where a scalar dark soliton coexists with multiple incoherently coupled dark-bright vector solitons in the net normal cavity dispersion regime. Horizontal axis (upper trace); vertical axis (lower trace).

solitons and confirmed that if the effective gain bandwidth is negligible, the formed dark-bright vector solitons mimic the features of the NLSE solitons. Otherwise, the formed dissipative dark-bright vector solitons no longer possess the attraction feature. Our numerical results are well confirmed by the experimental investigations. Our research shows that a vector cavity SMF laser is an excellent experimental test-bed both for the NLSE and GLE types of vector soliton study.

ACKNOWLEDGMENTS

This work is supported partially by the Minister of Education (MOE), Singapore (Project No. 2018-T1-001-145), A*Star AME IRG (Project No. A1883c0003); National Natural Science Foundation of China (NSFC) (Grants No. 61875078 and No. 11704259), and Priority Academic Program Development of Jiangsu High Education Institutions (PAPD).

-
- [1] J. Ma, G. D. Shao, Y. F. Song, L. M. Zhao, Y. J. Xiang, D. Y. Shen, M. Richardson, and D. Y. Tang, Observation of dark-bright vector solitons in fiber lasers, *Opt. Lett.* **44**, 2185 (2019).
 - [2] X. Hu, J. Guo, G. D. Shao, Y. F. Song, S. W. Yoo, B. A. Malomed, and D. Y. Tang, Observation of incoherently coupled dark-bright vector solitons in single-mode fibers, *Opt. Express* **27**, 18311 (2019).
 - [3] D. N. Christodoulides, Black and white vector solitons in weakly birefringent optical fibers, *Phys. Lett. A* **132**, 451 (1988).
 - [4] M. Lisak, A. Hook, and D. Anderson, Symbiotic solitary-wave pairs sustained by cross-phase modulation in optical fibers, *J. Opt. Soc. Am. B* **7**, 810 (1990).
 - [5] M. Haelterman and A. P. Sheppard, Polarization domain walls in diffractive or dispersive Kerr media, *Opt. Lett.* **19**, 96 (1994).
 - [6] S. Trillo, S. Wabnitz, E. M. Wright, and G. I. Stegeman, Optical solitary waves induced by cross-phase modulation, *Opt. Lett.* **13**, 871 (1988).
 - [7] A. V. Buryak, Y. S. Kivshar, and D. F. Parker, Coupling between dark and bright solitons, *Phys. Lett. A* **215**, 57 (1996).
 - [8] V. V. Afanasjev, Y. S. Kivshar, V. V. Konotop, and V. N. Serkin, Dynamics of coupled dark and bright optical solitons, *Opt. Lett.* **14**, 805 (1989).
 - [9] D. Y. Tang, J. Guo, Y. F. Song, G. D. Shao, L. M. Zhao, and D. Y. Shen, Temporal cavity soliton formation in an anomalous dispersion cavity fiber laser, *J. Opt. Soc. Am. B* **31**, 3050 (2014).
 - [10] P. Grelu and N. Akhmediev, Dissipative solitons for mode-locked lasers, *Nat. Photonics* **6**, 84 (2012).
 - [11] M. Mirzazadeh, M. Ekici, A. Sonmezoglu, M. Eslami, Q. Zhou, A. H. Kara, D. Milovic, F. B. Majid, A. Biswas, and M. Belic, Optical solitons with complex Ginzburg-Landau equation, *Nonlinear Dyn.* **85**, 1979 (2016).
 - [12] D. Y. Tang, L. M. Zhao, B. Zhao, and A. Q. Liu, Mechanism of multisoliton formation and soliton energy quantization in passively mode-locked fiber lasers, *Phys. Rev. A* **72**, 043816 (2005).
 - [13] H. Zhang, D. Y. Tang, L. M. Zhao, and N. Xiang, Coherent energy exchange between components of a vector soliton in fiber lasers, *Opt. Express* **16**, 12618 (2008).
 - [14] L. M. Zhao and D. Y. Tang, Generation of 15-nJ bunched noise-like pulses with 93-nm bandwidth in an erbium-doped fiber ring laser, *Appl. Phys. B* **83**, 553 (2006).
 - [15] L. M. Zhao, D. Y. Tang, and A. Q. Liu, Chaotic dynamics of a passively mode-locked soliton fiber ring laser, *Chaos* **16**, 013128 (2006).
 - [16] X. Hu, J. Guo, Y. F. Song, L. M. Zhao, L. Li, and D. Y. Tang, Dissipative Peregrine Solitons in fiber lasers, *J. Phys. Photonics* [to be published] (2020).
 - [17] K. Tai, A. Hasegawa, and A. Tomita, Observation of Modulational Instability in Optical Fibers, *Phys. Rev. Lett.* **56**, 135 (1986).
 - [18] S. Wabnitz, E. M. Wright, and G. I. Stegeman, Polarization instabilities of dark and bright coupled solitary waves in birefringent optical fibers, *Phys. Rev. A* **41**, 6415 (1990).
 - [19] V. S. Grigoryan and T. S. Muradyan, Evolution of light pulses into autosolitons in nonlinear amplifying media, *J. Opt. Soc. Am. B* **8**, 1757 (1991).
 - [20] G. D. Shao, Y. F. Song, L. M. Zhao, D. Y. Shen, and D. Y. Tang, Soliton-dark pulse pair formation in birefringent cavity fiber lasers through cross phase coupling, *Opt. Express* **23**, 26252 (2015).